

Article

Acetylcholinesterase Immobilization on ZIF-8/Graphene Composite Engenders High Sensitivity Electrochemical Sensing for Organophosphorus Pesticides

Long Wen [†], Ning Wang [†], Zhuoliang Liu ^{*ID}, Cheng-an Tao ^{ID}, Xiaorong Zou, Fang Wang and Jianfang Wang ^{*ID}

College of Science, National University of Defense Technology, Changsha 410073, China

^{*} Correspondence: hemazaizai@163.com (Z.L.); wangjianfang@nudt.edu.cn (J.W.)[†] These authors contributed equally to this work.

Abstract: A sensitive and flexible detection method for organophosphorus pesticides (OPs) detection is a crucial request to avoid their further expanded pollution. Herein, an acetylcholinesterase (AChE) electrochemical sensor, based on the co-modification of ZIF-8 and graphene (GR), was constructed for the detection of OPs. ZIF-8/GR composite can provide a stable and biocompatible environment for the loading of AChE and can accelerate the chemical reaction on the electrode surface. After optimization, the linear detection range of the constructed AChE-CS/GR/ZIF-8/GCE sensor for ICP was 0.5–100 ng/mL (1.73–345.7 nM), and the limit of detection was 0.18 ng/mL (0.62 nM). Moreover, high sensitivity and high specificity of the sensor were also achieved in actual cabbage and tap water samples. Therefore, it has great potential for the application of organophosphorus pesticide residue analysis.



Citation: Wen, L.; Wang, N.; Liu, Z.; Tao, C.-a.; Zou, X.; Wang, F.; Wang, J. Acetylcholinesterase Immobilization on ZIF-8/Graphene Composite Engenders High Sensitivity Electrochemical Sensing for Organophosphorus Pesticides.

Chemosensors **2022**, *10*, 418.
<https://doi.org/10.3390/chemosensors10100418>

Academic Editors: Yue Yi, Yong Jiang, Guofeng Cui and Mingfei Pan

Received: 11 September 2022

Accepted: 10 October 2022

Published: 13 October 2022

Publisher's Note: MDPI stays neutral with regard to jurisdictional claims in published maps and institutional affiliations.



Copyright: © 2022 by the authors. Licensee MDPI, Basel, Switzerland. This article is an open access article distributed under the terms and conditions of the Creative Commons Attribution (CC BY) license (<https://creativecommons.org/licenses/by/4.0/>).

Keywords: electrochemical biosensor; metal-organic framework; graphene; acetylcholinesterase; isocarbophos

1. Introduction

Organophosphorus pesticides (chlorpyrifos, methylparathion, isocarbophos, etc.) used in agricultural production have been extremely harmful to the environment and humans, due to their high toxicity, even at very low concentrations. The organophosphorus compounds induce human poisoning through strong inhibition of acetylcholinesterase (AChE) activity, causing the accumulation of acetylcholine (ACh) in the body to lead to acute poisoning with serious disorders of the nervous system and even death [1,2], which reminds us that research on effective organophosphorus pesticide defense and rapid detection methods is still worthwhile and urgent.

Traditional analytical methods for OPs are mainly based on chromatography, including high-performance liquid chromatography (HPLC) [3], gas-liquid chromatography-mass spectrometry (GC-MS) [4], and high-performance liquid chromatography-mass spectrometry (HPLC-MS) [5]. Although these analysis methods have high sensitivity and accuracy, they are complex, expensive, and difficult to operate, which limits these methods in the practical application of OPs detection [6]. However, electrochemical biosensors combining biological characteristic elements with electrochemistry have high applicability because of their high sensitivity, low cost, small size, ease to operate, fast detection, and direct detection in the field [7].

Among them, enzyme electrochemical biosensors using AChE as the recognition element are widely used for OPs detection [8]. However, the immobilization of enzymes has always been an important factor affecting the performance of enzyme sensors. Introducing suitable nanomaterials to increase the enzyme loading, without losing its activity, is a widely used idea [9–11]. Metal-organic frameworks (MOFs) are a class of porous nanomaterials prepared by bridging metal ions or metal clusters with organic ligands. Due to their diverse

structure, adjustable pore size, large specific surface area, and good adsorption affinity, they are widely used in the field of biosensing [12–14]. Zeolitic imidazolate frameworks (ZIFs), as a special subfamily of MOFs, consist of transition metal ions and imidazole or imidazole derivatives coordination [15], where ZIF-8 materials are made by combining Zn^{2+} and dimethylimidazole. In addition to the above advantages, ZIF-8 has good biocompatibility, because the Zn^{2+} imidazole ester group is a component of the physiological system [16]. Moreover, ZIF-8 has excellent chemical resistance, maintaining good crystallinity and porosity, even after a period of time, in solvents, such as water, methanol, ethanol, and N,N-dimethylformamide (DMF) [17]. Therefore, it is well-suited as a carrier for biosensitive substances [18–20]. Many of the literature have reported the embedding of enzymes in the pore structure of ZIFs [21,22]. For enzymes, especially AChE with complex conformation and deep active center, being immobilized in the interior of MOFs is not necessarily the most advantageous. Small pores may limit the access of the substrate to the active center of the enzyme and affect the catalytic efficiency of the enzyme. Li's group created a hollow covalent organic framework (COF) capsule constructed for enzyme encapsulation using MOF as a sacrificial template. Compared to enzymes assembled on electrodes, the enzyme@COF microcapsules exhibited good stability and ensured enzyme conformational expansion [23]. However, this method involves multiple steps, such as encapsulation and etching, which are complicated to operate. How to achieve both simple and efficient enzyme electrode construction is still in need of further research.

Inspired by the above concept, we used ZIF-8 as a substrate to immobilize the enzyme, expecting to increase the enzyme loading, while maximizing the enzyme activity by simply mixing and loading the enzyme on the periphery of ZIF-8. The direct mixing process would preserve the original conformation of AChE and make the substrates more easily approach the active center of the enzyme. Therefore, this work is a representative for the study of sensors based on 3D MOFs surface immobilization of AChE. Due to the poor conductivity of MOF, we also introduced graphene to improve the electron transfer efficiency. After optimization, the sensor constructed with ZIF-8/GR composite showed good performance and successfully achieved the detection of ICP in vegetable and tap water samples, demonstrating the feasibility of the method and its great potential application in the analysis of organophosphorus pesticide residues.

2. Experimental Section

2.1. Chemicals and Reagents

Acetylcholinesterase (AChE, EC3.1.1.7, C3389-500UN), acetylthiocholine chloride (ATCl, A5626), and isocarbophos (ICP, 37901-100MG) were purchased from Sigma Aldrich (Saint Louis, MS, USA). Potassium ferricyanide ($\text{K}_3[\text{Fe}(\text{CN})_6]$) and potassium ferrocyanide ($\text{K}_4[\text{Fe}(\text{CN})_6] \cdot 3\text{H}_2\text{O}$) were purchased from Guangfu Technology Development Co., Ltd. (Tianjin, China). Potassium chloride (KCl), sodium dihydrogen phosphate ($\text{NaH}_2\text{PO}_4 \cdot 2\text{H}_2\text{O}$), disodium hydrogen phosphate ($\text{Na}_2\text{HPO}_4 \cdot 12\text{H}_2\text{O}$), and chitosan (CS) were purchased from Sinopharm Chemical Reagent Beijing Co., Ltd. (Beijing, China). Zinc nitrate ($\text{Zn}(\text{NO}_3)_2$) was purchased from Xilong Science Co., Ltd. (Shantou, China), 2-Methylimidazole (2-MI) was purchased from Maclean Biochemical Technology Co., Ltd. (Shanghai, China). Monolayer graphene dispersion was purchased from Suzhou Tanfeng Graphene Technology Co., Ltd. (Suzhou, China). The glassy carbon electrodes were purchased from Ada Hengcheng Technology Development Co., Ltd. (Tianjin, China). All other chemicals and reagents used in this study were of analytical grade, and all aqueous solutions were prepared with ultrapure water ($18.25 \text{ M}\Omega/\text{cm}$) by a Millipore Direct-Q water system.

2.2. Instruments and Measurements

XRD (MxiniFlex600cx, Rigaku; Tokyo, Japan) was used to verify the crystal structure, and purity of ZIF-8, FT-IR (Spectrum Two, PerkinElmer, Waltham, MA, USA) was used to characterize the chemical structure of ZIF-8. SEM (Sigma300, Zeiss, Oberkochen, Germany) photographed the microscopic surface morphologies of ZIF-8 and GR. All electrochem-

ical tests were carried out on Electrochemical Workstation (CHI760E, CH Instruments; Shanghai, China).

2.3. Synthesis of AChE-CS/GR/ZIF-8 Composites

Zinc nitrate (1.98 mM) was dissolved in 40 mL deionized water, and then the above solution was added to 138.2 mM of 2-MI (molar ratio 1:70). The solution was stirred at 1000 rpm for 2 h at room temperature and then filtered. The collected particles were washed three times with deionized water. Finally, the product was dried in a vacuum drying oven at 80 °C for 10 h and ground into fine particles.

ZIF-8 were uniformly dispersed in PBS buffer (pH = 7.4) for 30 min. A liquid transfer gun was used to take 2 µL ZIF-8 dispersion (3.5 mg/mL) and 2 µL graphene dispersion (4 µg/mL), and then 2 µL 0.2 U/µL AChE buffer solution and 0.2% chitosan (CS) solution of pH 5.0 were added into a 0.5 mL centrifuge tube, respectively. The liquid in the centrifuge tube was mixed evenly using a vibration mixer shaking for 30 s. Thus, the AChE-CS/GR/ZIF-8 composites were synthesized.

2.4. Fabrication of Electrochemical Enzyme Biosensor

Glassy carbon electrode (GCE) needs to be polished and cleaned before use. The specific process is as follows: polish the GCE with 1.0 µm, 0.3 µm, and 0.05 µm alumina powder, respectively, then ultrasonic clean in deionized water, ethanol, and deionized water, respectively (time should not be too long to avoid electrode damage). Finally, the electrode surface was dried with nitrogen gas.

The AChE-CS/GR/ZIF-8/GCE sensor was obtained by evenly dropping the above 7 µL mixture onto the surface of GCE with a pipette gun and then dried in a refrigerator at 4 °C for 4 h.

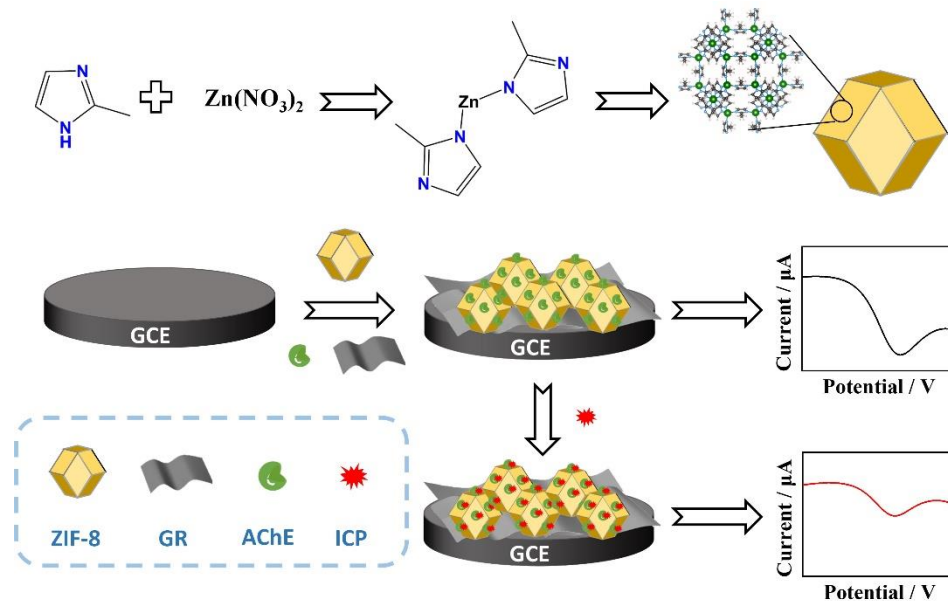
2.5. Electrochemical Measurement

Cyclic voltammetry (CV), alternating impedance spectroscopy (EIS), and differential pulse voltammetry (DPV) tests were performed on the prepared AChE-CS/GR/ZIF-8/GCE sensor. CV tests were carried out in a mixture of solutions containing 0.1 M KCl and 5 mM $K_3[Fe(CN)_6]/K_4[Fe(CN)_6]$ (1:1), the scan speed was set to 50 mV/s, and the voltage range is −0.2–0.6 V. The EIS test solution is the same as CV, the test frequency was 0.01–100 kHz, the initial potential was 0.23 V, and the amplitude was 5 mV. These two measurements were used to characterize the effect of different material modifications on the enzyme electrode.

DPV assays were performed in PBS containing 1 mM ATCl. The test voltage range was 0.3–0.9 V, the pulse width was 50 ms, the voltage increment was 4 mV, and the rest time was 2 s. The detection of AChE-CS/GR/ZIF-8/GCE sensor was based on the change of DPV response current. The detection principle is shown in Scheme 1. Acetylthiocholine chloride (ATCl), as a substrate, can be hydrolyzed into acetate and thiocholine (TCl) under the catalysis of AChE. TCl can be further oxidized under a certain voltage to generate an oxidation current, and the magnitude of the current is related to its concentration. When ICP exists, it can combine with AChE to form phosphorylated AChE, thereby inhibiting the activity of AChE, reducing the production of TCl, and reducing the oxidative current. In a certain range, the inhibition of AChE by ICP is linear with its concentration, so it can be quantitatively analyzed. The inhibition rate was calculated as follows:

$$\text{Inhibition(\%)} = \frac{I_0 - I_1}{I_0} \times 100\%,$$

where I_0 is the initial DPV peak current of the sensor, and I_1 is the DPV peak current of the sensor after a certain concentration of ICP inhibition.



Scheme 1. Schematic diagram of the construction of the AChE-CS/GR/ZIF-8/GCE sensor for ICP detection.

2.6. Detection of Isocarbophos in Real Samples

A total of 1.0 g/L ICP standard solution was prepared with acetone and diluted with ultra-pure water to obtain working standard solutions of different concentrations. Fresh cabbages were purchased from the local market. The cabbage was cut into small pieces of approximately 2 cm × 2 cm with scissors, weighed to 20 g, and further pounded in a mortar and pestle. The mixture of 20 mL of deionized water and acetone (1:1) was shaken for 10 min and filtered by ultrasonic stirring for 30 min. Finally, the acetone in the filtrate was removed by rotary evaporation at 60 °C, and the remaining filtrate was diluted 100 times to obtain the final cabbage leachate sample. Different concentrations of ICP standards were added to it to make spiked samples. Three measurements were made using different sensors, and the corresponding concentration values were obtained from the standard curve. It was divided by the actual spiked concentration to calculate the recovery of the sample. Alternatively, ICP standards were added directly to the tap water samples to make spiked samples, and the testing procedure was the same as above.

2.7. Limit of Detection

The limit of detection (LoD) represents the concentration C_L corresponding to the minimum analytical signal X_L that the electrode can reasonably detect [24]. The calculation formula is as follows:

$$X_L = \bar{X} + KS$$

where X_L is the minimum analytical signal, \bar{X} is the mean value of the blank, S is the standard deviation of the blank, and K is a constant related to the confidence level, generally taken as 3. Therefore, the C_L corresponds to the value calculated by the calibration plot obtained from a given analytical procedure.

3. Results and Discussion

3.1. Characterization of Nanomaterials

The composites were characterized by SEM. Figure 1a shows the morphology of ZIF-8, observing a distinct rhombic dodecahedral shape, with a particle size of about 100–200 nm. Figure 1b demonstrates the presence of a large number of structural defects and folds on the GR surface. In addition to its inherent advantage of high electrical conductivity, it also provides sufficient attachment points for ZIF-8 and AChE, which is confirmed by the

ZIF-8/GR morphology shown in Figure 1c. Finally, a CS film wrapping the composite can be observed in Figure 1d, further solidifying the loading of the composite on the electrode surface.

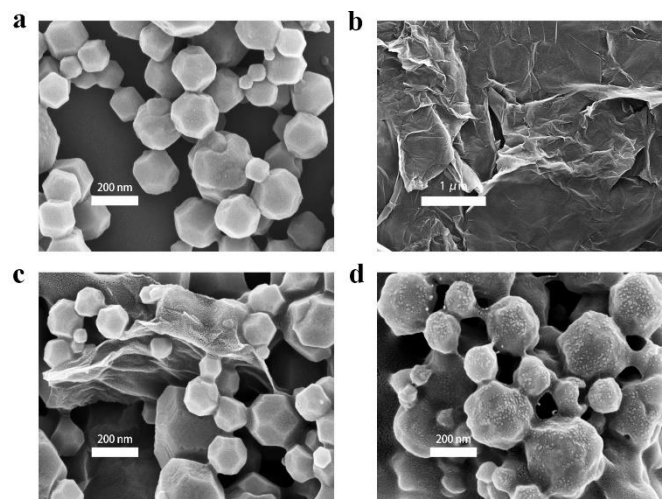


Figure 1. SEM image of (a) ZIF-8, (b) GR, (c) ZIF-8/GR, and (d) ZIF-8/GR/AChE-CS.

Figure 2a shows the XRD image of ZIF-8 particles. The characteristic peaks of ZIF-8 crystals are sharp and free of other spurious peaks, which are in general agreement with the XRD simulated images, implying that the ZIF-8 particles have good purity and crystallinity. FT-IR (Figure 2b) shows that there is an absorption peak at 1583 cm^{-1} for the stretching vibration absorption peak of the C=N bond. In addition, the sample shows an absorption peak at 420 cm^{-1} , attributed to the stretching vibration peak of Zn-N. We also found that the synthesized samples did not show the stretching vibration peak of the N-H bond in 2-MI at $2500\text{--}2800\text{ cm}^{-1}$ and 1851 cm^{-1} , which can indicate that the 2-MI in the synthesized products has been completely deprotonated [25]. The above results indicate that ZIF-8 nanoparticles with good morphology and structure have been successfully prepared.

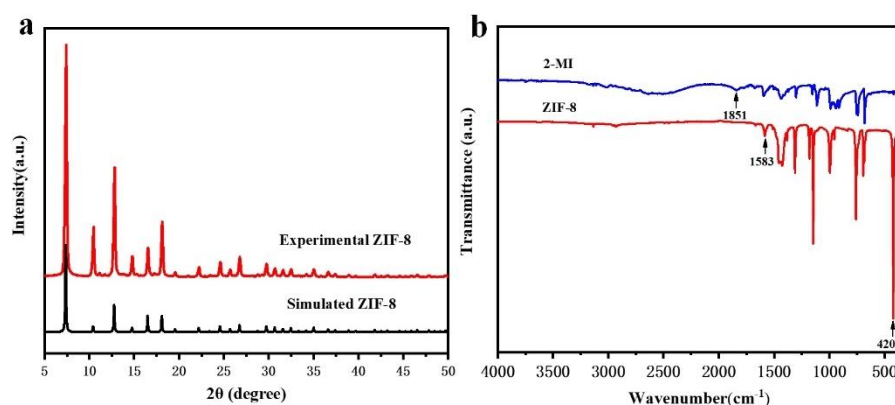


Figure 2. (a) XRD patterns of ZIF-8, (b) FT-IR spectrum of ZIF-8 and 2-MI.

3.2. Electrochemical Characterization of Enzyme Biosensor

The electrochemical characteristics of electrodes modified with different materials were investigated by CV and EIS. Figure 3a shows that the CV of each electrode exhibits a pair of reversible redox peaks. The bare glassy carbon electrode has strong redox peaks. After adding ZIF-8, the redox current decreased, which was caused by the poor conductivity of ZIF-8. While the electrode was modified by GR, the redox current was significantly increased because its good electrical conductivity accelerated the electron transfer. After loading AChE/CS, the redox current decreased again, mainly caused by the poor conduc-

tivity of acetylcholinesterase as a protein molecule and hindrance of CS membrane, these factors hinder the redox electric probes diffusion and electron transferring.

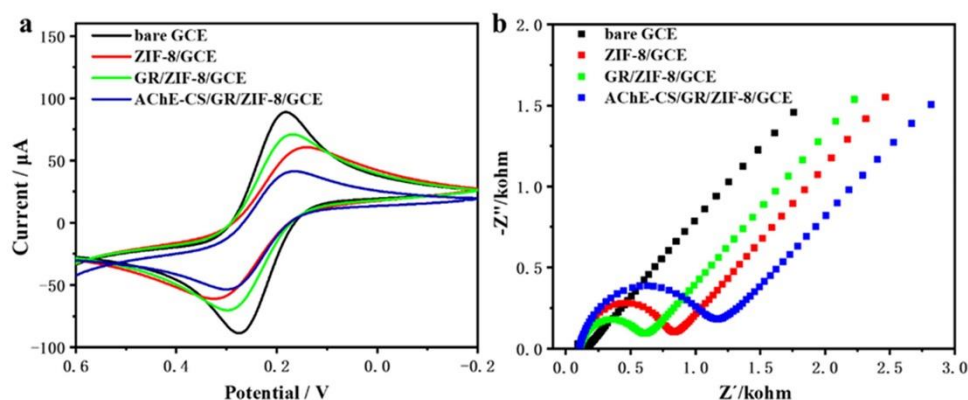


Figure 3. CV curves (a) and Nyquist diagrams (b) of different modified electrodes in 5 mM $\text{Fe}(\text{CN})_6^{3-/4-}$ (1:1) test solution containing 0.1 M KCl.

EIS can be used to probe the interface properties of electrodes during different modification processes. A typical Nyquist plot consists of a high-frequency semicircular region associated with electron transfer-limited processes and a low-frequency linear part associated with diffusion-limited processes. The diameter of the semicircle is often used to estimate the resistance of charge transfer (Rct). In Figure 3b, the Rct of the bare glassy carbon electrode is 74.5 Ω . The Rct of ZIF-8/GCE was significantly increased to 677 Ω . After adding GR, Rct dropped to 470.9 Ω . Finally, the loading of AChE-CS increased Rct to 981.2 Ω . The conclusion of the EIS test is consistent with the CV study, and the above results show that the composites were successfully loaded on the electrodes.

3.3. Study on Substrate Response of Different Enzyme Electrodes

AChE-CS/GCE, AChE-CS/ZIF-8/GCE, and AChE-CS/GR/ZIF-8/GCE were constructed by the same method, and the responses of different enzyme electrodes to the substrate ATCl were investigated by DPV. Figure 4 shows that all three electrodes have obvious oxidation peaks around 0.65 V, which are generated by the electrochemical oxidation of ATCl hydrolysis product TCl. By comparing the differences of the three response currents, it can be found that the sensor constructed with bare GCE electrodes generates the smallest response current, and the response current increases significantly after adding ZIF-8 and further increases after adding GR. The above experimental results show that the ZIF-8/GR composites can effectively immobilize AChE and improve the electron transfer rate, thereby increasing the response current of the sensor, which is beneficial to improve the sensor performance.

3.4. Optimization of Detection Conditions of Enzyme Biosensor

In order to detect ICP more efficiently and sensitively, we optimized several key influencing factors related to sensor performance, including the amount of AChE loading, the concentration of ZIF-8, and the concentration of GR. A series of sensors with different AChE loadings (0.1 U–0.7 U) were prepared. Their DPV response current magnitudes at 1 mM ATCl were compared. As shown in Figure 5a, the response current increases with increasing AChE loading, in the range of 0.1 U–0.4 U. The response current reaches a maximum when the AChE activity is 0.4 U. The response current decreases when the acetylcholinesterase content increases further. This is due to the low ability of a small amount of AChE to catalyze the ATCl hydrolysis reaction, and the response current is relatively small. However, since the active center of AChE is deep in its structure, too much loading does not allow AChE to perform more effective catalysis, but may lead to poor conductivity of the electrode. Therefore, 0.4 U was chosen as the optimal loading for constructing the sensor.

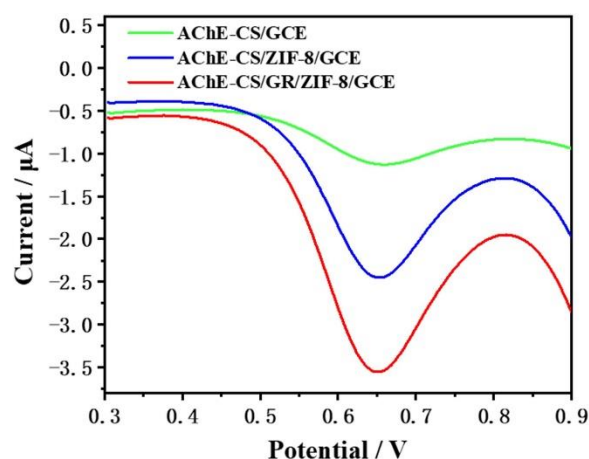


Figure 4. DPV response curves of enzyme electrodes modified with different nanomaterials in 0.1 M PBS buffer solution containing 1 mM ATCl.

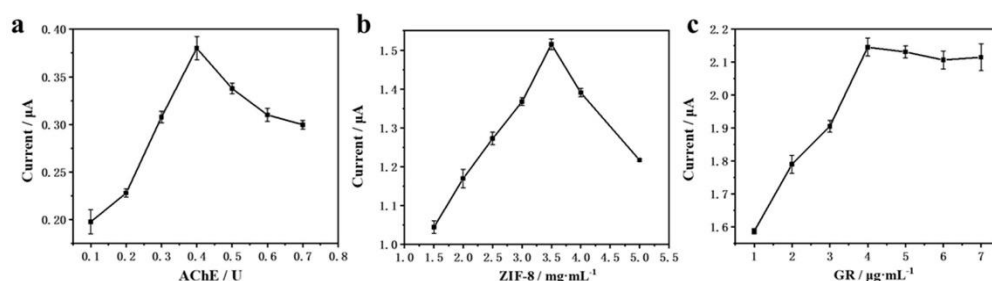


Figure 5. The trend of the response current of different sensors to 1 mM ATCl of (a) different AChE loads, (b) different ZIF-8 concentration, (c) different GR concentration.

The concentration of ZIF-8 is also directly related to the sensing performance of the AChE sensor. A series of ZIF-8 dispersions with different concentrations were prepared for the construction of the AChE sensor, and its DPV response current to 1 mM substrate ATCl was observed and recorded; the experimental results are shown in Figure 5b, and they reached the maximum at 3.5 mg/mL. This is mainly due to the adsorption of ZIF-8, which provides a stable environment for AChE, but the excessive amount of ZIF-8 will lead to the poor conductivity of the electrode, which is not conducive to electron transfer. Therefore, 3.5 mg/mL was used as the optimum concentration value in the subsequent experiments.

In addition, the effect of GR concentration on the response current of DPV was also investigated. It can be found from Figure 5c that the response current increased with the increase of GR concentration at the beginning, but after the GR concentration reached 4 µg/mL, the response current remained basically stable when the GR concentration was increased again. This is due to the good electrical conductivity of GR, and the appropriate amount of GR can effectively promote the electron transfer and enhance the AChE-catalyzed hydrolysis reaction. Therefore, 4 µg/mL was chosen as the optimum concentration.

3.5. The Performance of AChE-CS/GR/ZIF-8/GCE Electrochemical Biosensor

The performance of the AChE-CS/GR/ZIF-8/GCE sensor for ICP detection was investigated under optimal experimental conditions (the loading of AChE is 0.4 U, the concentration of ZIF-8 is 3.5 mg/mL, and the concentration of GR is 4 µg/mL). Figure 6a shows that the DPV response current decreases with increasing ICP concentration. According to the linear calibration curve of DPV response current suppression versus the logarithm of ICP concentration in Figure 6b, it can be found that the AChE-CS/GR/ZIF-8/GCE sensor shows a linear relationship between the suppression rate and the logarithm of ICP concentration after 15 min of suppression in ICP at 0.5, 1, 5, 10, 50, and 100 ng/mL concentrations. The linear fitting equation was $I(\%) = 0.143 \lg C_{\text{ICP}} + 0.284$, $R^2 = 0.995$.

Therefore, the linear detection range of the AChE-CS/GR/ZIF-8/GCE sensor for ICP in this paper was 0.5–100 ng/mL (1.73–345.7 nM), and the LoD was calculated to be 0.18 ng/mL (0.62 nM).

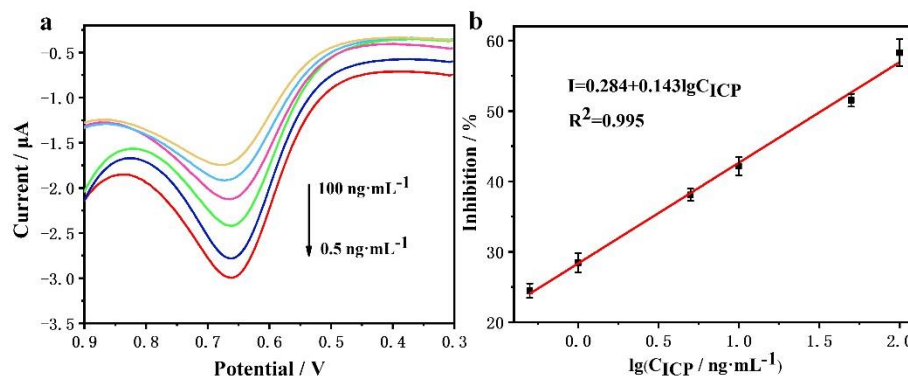


Figure 6. (a) DPV response of AChE-CS/GR/ZIF-8/GCE after ICP inhibition at different concentrations (0.5, 1, 5, 10, 50, 100 ng/mL) in 1 mM ATCl PBS solution. (b) Calibration curve of inhibition rate and the logarithm of ICP concentration.

Since there are few studies using AChE sensors to detect ICP, a fraction of AChE sensors detecting other OPs were used for comparison. As shown in Table 1, the sensor proposed in this work has a comparable, even wider, linear range and lower detection limits than them.

Table 1. Comparison of the performance of some other reported AChE sensors for the detection of OPs.

Method	Target	Linear Range	Detection Limit	Ref.
GN-AuNPs/CLDH-AChE/GCE	Chlorpyrifos	0.1426–427.87 μ M	142.6 nM	[26]
AChE-MWCNTs-Au-CHIT/GCE	Malathion	3.027–3027 nM	1.8 nM	[27]
AChE-Cs/Pd-Cu NWS/GCE	Malathion	15 pM–9 μ M	4.5 pM	[28]
AChE/CNT-NH ₂ /GCE	Paraoxon	0.2–1 nM, 1–30 nM	0.08 nM	[29]
Nafion-AChE/PB/DSPE	Isocarbophos	0.35–17.3 μ M	1.73 μ M	[30]
AChE-CS/GR/ZIF-8/GCE	Isocarbophos	1.73–345.7 nM	0.62 nM	This work

3.6. Anti-Interference and Reproducibility of Enzyme Sensor

Glucose, urea, CO₃²⁻, Mg²⁺, and NO₃⁻, which are common interfering substances in practical assays, were selected. Their concentrations were set to 5 times the substrate concentrations for the anti-interference experiments. The PBS solution containing only 1 mM ATCl was used as the control group for the blank experiment. As can be seen in Figure 7a, the response current of the sensor did not change significantly in the solutions containing glucose, CO₃²⁻, and Mg²⁺ interfering substances, while the response current values decreased slightly in the solutions containing urea and NO₃⁻ interfering substances, proving the good anti-interference ability of the sensor.

Repeatability is also an important index to evaluate the sensor performance. Five identical sensors were prepared in parallel to test the DPV response current in 1 mM ATCl in PBS solution. As shown in Figure 7b, the relative standard deviation (RSD) for the five electrodes was 5.05%, which indicates that the sensor has good reproducibility.

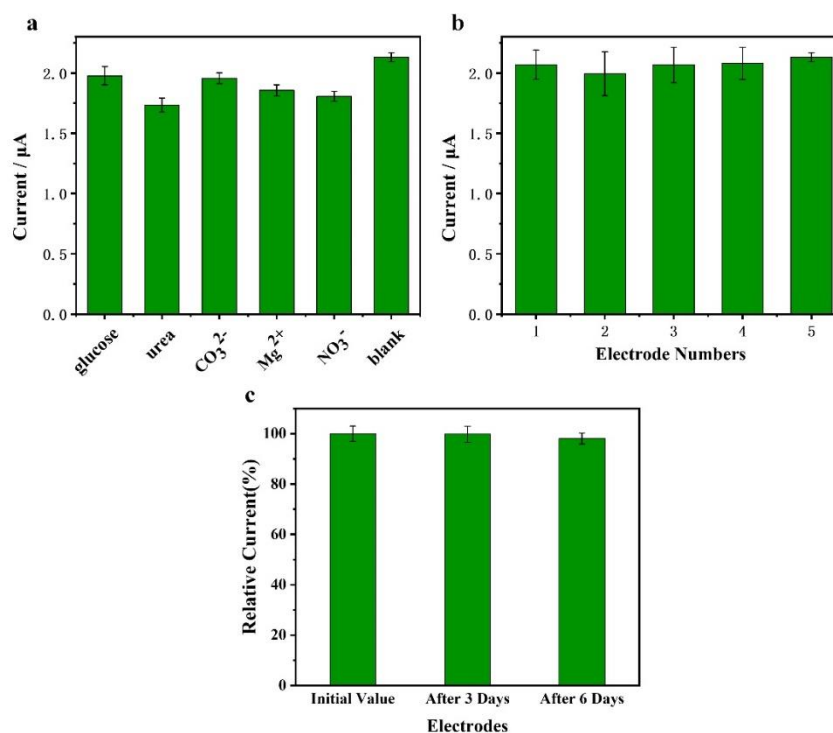


Figure 7. (a) Anti-interference, (b) Repeatability, (c) Stability tests of AChE-CS/GR/ZIF-8/GCE sensor.

Experiments on the preservation stability of the sensor were implemented, and the results were shown in the modified Figure 7c, where we stored the prepared AChE-CS/GR/ZIF-8/GCE sensors in a refrigerator at 4 °C. After 3 days, the sensors maintained 99.79% of the initial response current. After 6 days, the response of the sensors retained 98.09% of the initial response current. The test results of three parallel prepared sensors were used as a reference for each time point. The results indicate that the sensor has good preservation stability during the experimental period.

3.7. Real Samples Detection

Cabbage and tap water samples were selected for ICP recovery studies to validate the practical application of the sensor AChE-CS/GR/ZIF-8/GCE. To make the analysis more comprehensive, three concentrations were set within the detection range of the sensor (0.001, 0.01, and 0.1 µg/mL). As shown in Table 2, the recoveries of cabbage samples and tap water ranged from 88.1% to 122.4%, and the relative standard deviations ranged from 1.7% to 5.6%. The results indicate that the sensor is acceptable for the detection of ICP in real samples and has a promising development in the field of food safety and water monitoring.

Table 2. Recovery results of the proposed AChE-CS/GR/ZIF-8/GCE electrochemical biosensor for detecting ICP in cabbage and tap water samples.

Sample	Added (µg/mL)	Found (µg/mL)	Recovery (%)	RSD (%)
Cabbage	0.001	0.00106	106.1	2.2
	0.01	0.00918	91.7	5.6
	0.1	0.11427	114.3	2.7
Tap water	0.001	0.00096	95.7	3.9
	0.01	0.00881	88.1	1.7
	0.1	0.12237	122.4	3.5

4. Conclusions

In summary, we successfully constructed a highly efficient electrochemical AChE biosensor based on ZIF-8/GR composite for OPs detection. The AChE loading amount, ZIF-8 addition concentration, and GR addition concentration were optimized, and the obtained sensor had a high linear detection range of (0.5~100 ng/mL (1.73~345.7 nM)) and a low detection limit (0.18 ng/mL (0.62 nM)). In addition, it had good reproducibility, interference resistance, and storage stability. Satisfactory results were also obtained in the recovery studies of cabbage and tap water samples. The successful construction of the AChE-CS/GR/ZIF-8/GCE biosensor provides a simple and effective method for loading and modification of AChE on electrodes, which is valuable in the rapid detection of OPs.

Author Contributions: Conceptualization, Z.L. and J.W.; methodology, L.W., N.W., Z.L. and C.-a.T.; software and formal analysis, L.W. and N.W.; investigation, C.-a.T., X.Z., and F.W.; resources, X.Z. and F.W.; data curation, L.W. and N.W.; writing—original draft preparation, L.W. and N.W.; writing—review and editing, J.W., Z.L., C.-a.T., X.Z. and F.W.; supervision, Z.L., J.W. and C.-a.T.; project administration, Z.L. and J.W. All authors have read and agreed to the published version of the manuscript.

Funding: This research received funding from Independent Scientific Research Project of National University of Defense Technology (ZZKY-YX-09-04) and National Natural Science Foundation of China (21705163).

Institutional Review Board Statement: Not applicable.

Informed Consent Statement: Not applicable.

Data Availability Statement: Not applicable.

Acknowledgments: We thank for the funding of Independent Scientific Research Project of National University of Defense Technology (ZZKY-YX-09-04) and National Natural Science Foundation of China (21705163).

Conflicts of Interest: The authors declare that they have no known competing financial interest or personal relationships that could have appeared to influence the work reported in this paper.

References

1. John, H.; Thiermann, H. Poisoning by organophosphorus nerve agents and pesticides: An overview of the principle strategies and current progress of mass spectrometry-based procedures for verification. *J. Mass Spectrom. Adv. Clin. Lab* **2021**, *19*, 20–31. [[CrossRef](#)] [[PubMed](#)]
2. Vale, A.; Marrs, T.C.; Rice, P. Chemical terrorism and nerve agents. *Medicine* **2016**, *44*, 106–108. [[CrossRef](#)]
3. Catalá-Icardo, M.; Lahuerta-Zamora, L.; Torres-Cartas, S.; Meseguer-Lloret, S. Determination of organothiophosphorus pesticides in water by liquid chromatography and post-column chemiluminescence with cerium (IV). *J. Chromatogr. A* **2014**, *1341*, 31–40. [[CrossRef](#)]
4. Cacho, J.I.; Campillo, N.; Viñas, P.; Hernández-Córdoba, M. In situ ionic liquid dispersive liquid-liquid microextraction coupled to gas chromatography-mass spectrometry for the determination of organophosphorus pesticides. *J. Chromatogr. A* **2018**, *1559*, 95–101. [[CrossRef](#)] [[PubMed](#)]
5. Qi, P.; Wang, X.; Zhang, H.; Wang, X.; Xu, H.; Wang, Q. Rapid Enantioseparation and Determination of Isocarbophos Enantiomers in Orange Pulp, Peel, and Kumquat by Chiral HPLC-MS/MS. *Food Anal. Methods* **2015**, *8*, 531–538. [[CrossRef](#)]
6. Liu, M.; Wei, J.; Wang, Y.; Ouyang, H.; Fu, Z. Dopamine-functionalized upconversion nanoparticles as fluorescent sensors for organophosphorus pesticide analysis. *Talanta* **2019**, *195*, 706–712. [[CrossRef](#)] [[PubMed](#)]
7. Kordasht, H.K.; Pazhuhi, M.; Pashazadeh-Panahi, P.; Hasanzadeh, M.; Shadjou, N. Multifunctional aptasensors based on mesoporous silica nanoparticles as an efficient platform for bioanalytical applications: Recent advances. *TrAC Trends Anal. Chem.* **2020**, *124*, 115778. [[CrossRef](#)]
8. Rotariu, L.; Lagarde, F.; Jaffrezic-Renault, N.; Bala, C. Electrochemical biosensors for fast detection of food contaminants—Trends and perspective. *TrAC Trends Anal. Chem.* **2016**, *79*, 80–87. [[CrossRef](#)]
9. Meena, J.; Gupta, A.; Ahuja, R.; Singh, M.; Panda, A.K. Recent advances in nano-engineered approaches used for enzyme immobilization with enhanced activity. *J. Mol. Liq.* **2021**, *338*, 116602. [[CrossRef](#)]
10. Nemiwal, M.; Zhang, T.C.; Kumar, D. Enzyme immobilized nanomaterials as electrochemical biosensors for detection of biomolecules. *Enzyme Microb. Technol.* **2022**, *156*, 110006. [[CrossRef](#)] [[PubMed](#)]

11. Lu, J.; Nie, M.; Li, Y.; Zhu, H.; Shi, G. Design of composite nanosupports and applications thereof in enzyme immobilization: A review. *Colloids Surf. B Biointerfaces* **2022**, *217*, 112602. [[CrossRef](#)]
12. Slater, A.G.; Cooper, A.I. Function-led design of new porous materials. *Science* **2015**, *348*, 6238. [[CrossRef](#)]
13. Feng, Y.; Xu, Y.; Liu, S.; Wu, D.; Su, Z.; Chen, G.; Liu, J.; Li, G. Recent advances in enzyme immobilization based on novel porous framework materials and its applications in biosensing. *Coord. Chem. Rev.* **2022**, *459*, 214414. [[CrossRef](#)]
14. Daniel, M.; Mathew, G.; Anpo, M.; Neppolian, B. MOF based electrochemical sensors for the detection of physiologically relevant biomolecules: An overview. *Coord. Chem. Rev.* **2022**, *468*, 214627. [[CrossRef](#)]
15. Mohamud, M.A.; Yurtcan, A.B. Zeolitic imidazolate frameworks (ZIFs) derived porous carbon: A review from crystal growth & green synthesis to oxygen reduction reaction activity. *Int. J. Hydrog. Energy* **2021**, *46*, 33782–33800. [[CrossRef](#)]
16. Gao, L.; Chen, Q.; Gong, T.; Liu, J.; Li, C. Recent advancement of imidazolate framework (ZIF-8) based nanoformulations for synergistic tumor therapy. *Nanoscale* **2019**, *11*, 21030–21045. [[CrossRef](#)]
17. Park, K.S.; Zheng, N.; Cté, A.; Choi, J.Y.; Yaghi, O.M. Exceptional Chemical and Thermal Stability of Zeolitic Imidazolate Frameworks. *Proc. Natl. Acad. Sci. USA* **2006**, *103*, 10186–10191. [[CrossRef](#)]
18. Wang, Q.; Zhang, X.; Huang, L.; Zhang, Z.; Dong, S. GOx@ZIF-8(NiPd) Nanoflower: An Artificial Enzyme System for Tandem Catalysis. *Angew. Chem.* **2017**, *56*, 16082–16085. [[CrossRef](#)]
19. Ouyang, G.; Chen, G.; Huang, S.; Kou, X.; Wei, S.; Huang, S.; Jiang, S.; Shen, J.; Zhu, F. A Convenient and Versatile Amino-Acid-Boosted Biomimetic Strategy for the Nondestructive Encapsulation of Biomacromolecules within Metal–Organic Frameworks. *Angew. Chem. Int. Ed.* **2019**, *58*, 1463–1467. [[CrossRef](#)]
20. Wang, Y.; Hou, C.; Zhang, Y.; He, F.; Liu, M.; Li, X. Preparation of graphene nano-sheet bonded PDA/MOF microcapsules with immobilized glucose oxidase as a mimetic multi-enzyme system for electrochemical sensing of glucose. *J. Mater. Chem. B* **2016**, *4*, 3695–3702. [[CrossRef](#)]
21. Zhang, Q.; Zhang, L.; Dai, H.; Li, Z.; Fu, Y.; Li, Y. Biomineralization-mimetic preparation of robust metal-organic frameworks biocomposites film with high enzyme load for electrochemical biosensing. *J. Electroanal. Chem.* **2018**, *823*, 40–46. [[CrossRef](#)]
22. Wei, T.H.; Wu, S.H.; Huang, Y.D.; Lo, W.S.; Williams, B.P.; Chen, S.Y.; Yang, H.C.; Hsu, Y.S.; Lin, Z.Y.; Chen, X.H.; et al. Rapid mechanochemical encapsulation of biocatalysts into robust metal-organic frameworks. *Nat. Commun.* **2019**, *10*, 5002. [[CrossRef](#)] [[PubMed](#)]
23. Li, M.; Qiao, S.; Zheng, Y.; Andaloussi, Y.H.; Li, X.; Zhang, Z.; Li, A.; Cheng, P.; Ma, S.; Chen, Y. Fabricating covalent organic framework capsules with commodious microenvironment for enzymes. *J. Am. Chem. Soc.* **2020**, *142*, 6675–6681. [[CrossRef](#)] [[PubMed](#)]
24. Shrivastava, A.; Gupta, V. Methods for the determination of limit of detection and limit of quantitation of the analytical methods. *Chron. Young Sci.* **2011**, *2*, 21–25. [[CrossRef](#)]
25. Tran, U.; Le, K.; Phan, N. Expanding Applications of Metal–Organic Frameworks: Zeolite Imidazolate Framework ZIF-8 as an Efficient Heterogeneous Catalyst for the Knoevenagel Reaction. *ACS Catal.* **2011**, *1*, 120–127. [[CrossRef](#)]
26. Zhai, C.; Guo, Y.; Sun, X.; Zheng, Y.; Wang, X. An acetylcholinesterase biosensor based on graphene–gold nanocomposite and calcined layered double hydroxide. *Enzym. Microb. Technol.* **2014**, *58*, 8–13. [[CrossRef](#)]
27. Du, D.; Wang, M.; Cai, J.; Qin, Y.; Zhang, A. One-step synthesis of multiwalled carbon nanotubes-gold nanocomposites for fabricating amperometric acetylcholinesterase biosensor. *Sens. Actuators B Chem.* **2010**, *143*, 524–529. [[CrossRef](#)]
28. Song, D.; Li, Y.; Lu, X.; Sun, M.; Liu, H.; Yu, G.; Gao, F. Palladium-copper nanowires-based biosensor for the ultrasensitive detection of organophosphate pesticides. *Anal. Chim. Acta* **2017**, *982*, 168–175. [[CrossRef](#)]
29. Yu, G.; Wu, W.; Zhao, Q.; Wei, X.; Lu, Q. Efficient immobilization of acetylcholinesterase onto amino functionalized carbon nanotubes for the fabrication of high sensitive organophosphorus pesticides biosensors. *Biosens. Bioelectron.* **2015**, *68*, 288–294. [[CrossRef](#)]
30. Shi, Q.; Teng, Y.; Zhang, Y.; Liu, W. Rapid detection of organophosphorus pesticide residue on Prussian blue modified dual-channel screen-printed electrodes combining with portable potentiostat. *Chin. Chem. Lett.* **2018**, *29*, 1379–1382. [[CrossRef](#)]